# Supplementary Fig. 1

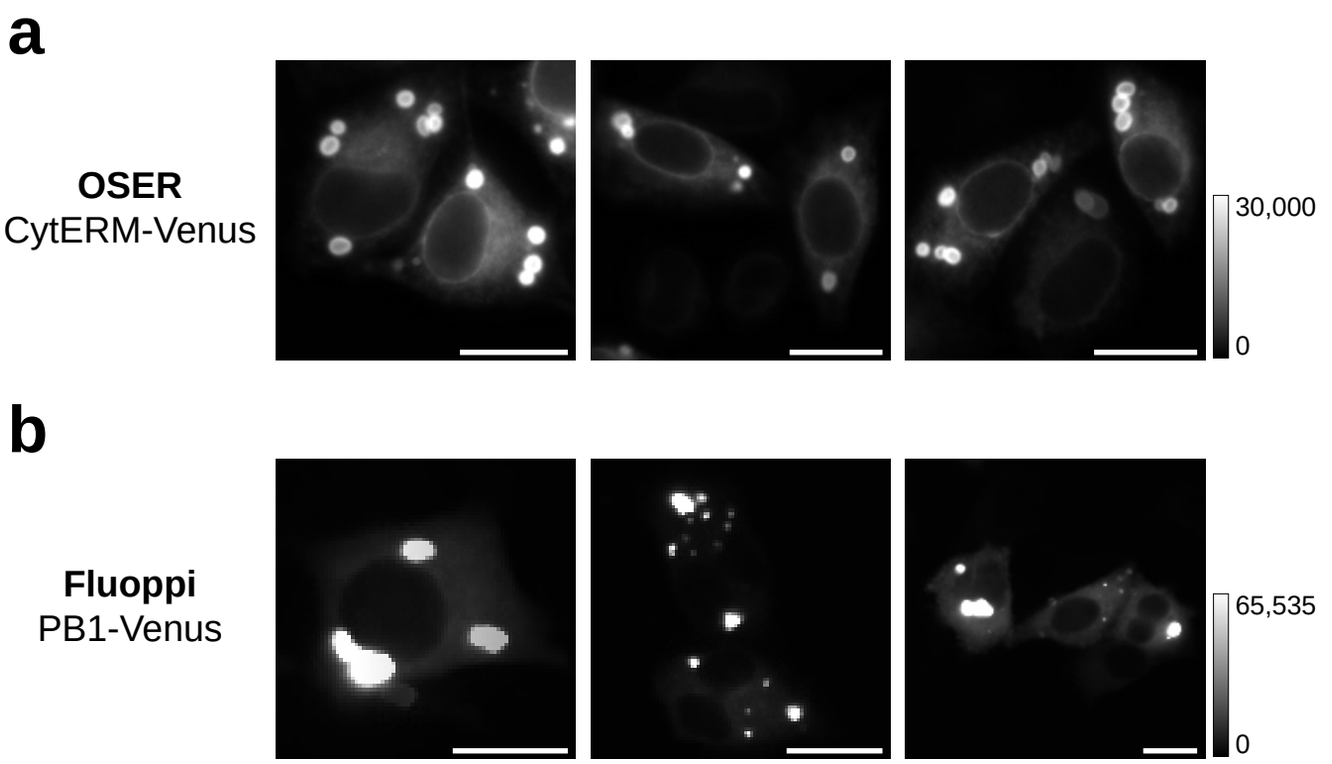


**Supplementary Fig. 1 | Comparison between OSER and Fluoppi for the assessment of Venus monomericity/dispersibility.**
**a,** OSER; three typical images of HeLa cells that showed whorls of CytERM-Venus signals.
**b,** Fluoppi; three typical images of HeLa cells that showed puncta of PB1-Venus signals. PB1-Venus appeared to yield more efficient signal concentration with less background than CytERM-Venus. Therefore, overall, Fluoppi is expected to provide a higher signal-to-noise ratio than OSER. Each gray scale indicates that the lowest and highest fluorescence intensities. Scale bars, 20 μm.

# Supplementary Fig. 2

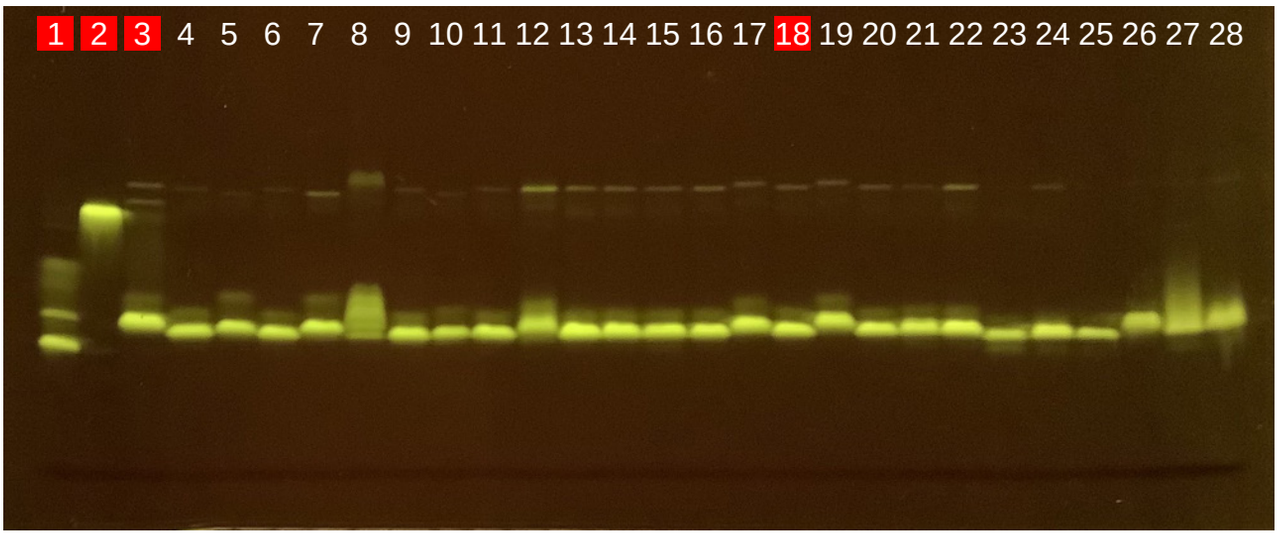


1) EGFP
2) StayGold
3) QC2-6
4) QC2-6 Y187F / R144I ran1
5) QC2-6 Y187F / R144I ran2
6) QC2-6 Y187F / R144I ran3
7) QC2-6 Y187F / R144I ran4
8) QC2-6 Y187F / R144I ran5
9) QC2-6 Y187F / R144I ran6
10) QC2-6 Y187F / R144I ran7
11) QC2-6 Y187F / R144I ran8
12) QC2-6 Y187F / R144I ran9
13) QC2-6 Y187F / R144I
14) QC2-6 Y187F / R144I / T155F
15) QC2-6 Y187F / R144I / T155H
16) QC2-6 Y187F / R144I / T155I
17) QC2-6 Y187F / R144I / T155K
18) QC2-6 Y187F / R144I / T155Q
19) QC2-6 Y187F / R144I / T155R
20) QC2-6 Y187F / R144I / T155V
21) QC2-6 Y187F / R144I / T155W
22) QC2-6 Y187F / R144I / T155Y
23) QC2-6 R144E
24) QC2-6 R144E / T155I
25) QC2-6 R144E / T155M
26) QC2-6 R144E / T155R
27) QC2-6 R144E / T155V
28) QC2-6 R144E / T155Y

**Supplementary Fig. 2 | Pseudonative SDS-PAGE of purified bacterially expressed proteins.**
A panel showing the final stage of the revolution reaching QC2-6 FIQ (lane 18). QC2-6 (lane 3) and its derivatives were analyzed in reference to EGFP (lane 1) and StayGold (lane 2). QC2-6 FIQ (= QC2-6 Y187F/R144I/T155Q) exhibited a slightly greater mobility than QC2-6. Lanes 4–12: nine bright colonies were selected from a mutant library on the basis of products of error-prone PCR on QC2-6 Y187F/R144I. ran: random mutagenesis.

# Supplementary Fig. 3

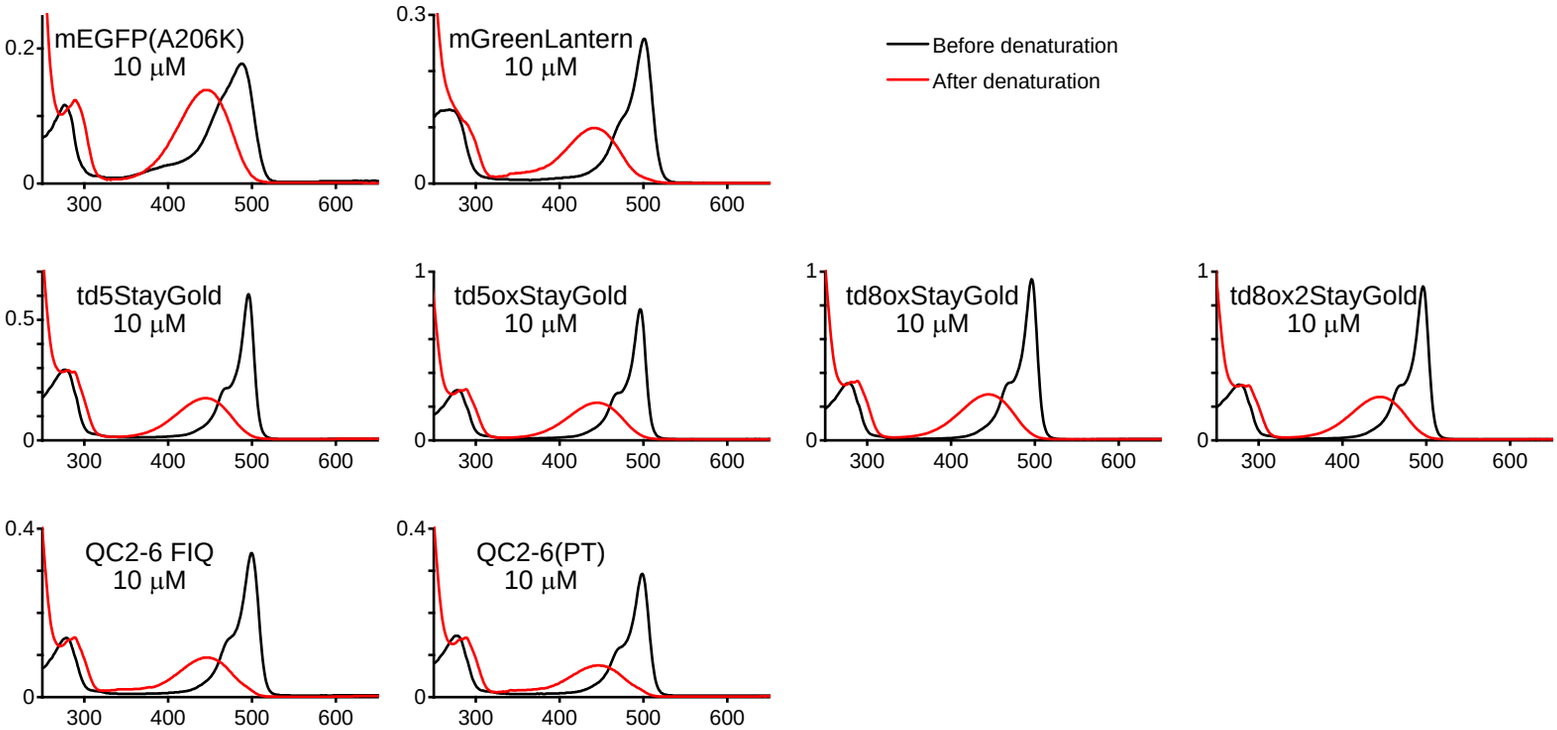


**Supplementary Fig. 3 | Spectral assessment of inherent qualities of FP chromophores.**
Absorption spectra of FPs before (black line) and after (red line) denaturation with 0.1 M NaOH. The FP concentration was 10 μM, and the path length was 1 cm. All these FPs carry X-Tyr-Gly, a chromophore-forming tripeptide, and their alkali-denatured chromophores contain a dehydrotyrosine residue conjugated to the imidazolone group and absorb light maximally at 447 nm with a molar extinction coefficient of 44,000 $M^{-1}$ $cm^{-1}$. This value was used for the determination of their absolute molar extinction coefficients.

# Supplementary Fig. 4

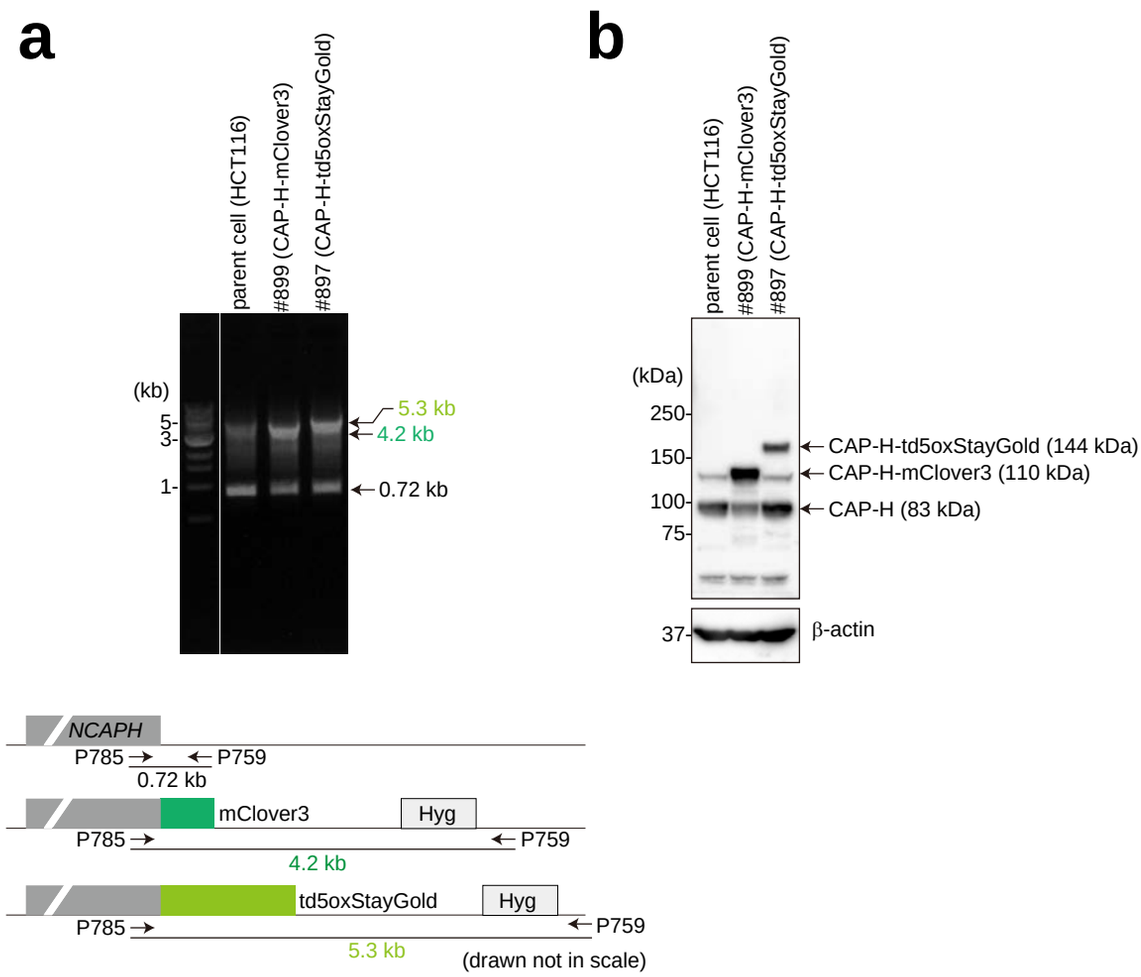


**Supplementary Fig. 4 | Validation of knock-in cell lines.**
Cell lines #899 and #897 were characterized in parallel with their parent (HCT116) by junction PCR (**a**) and western blotting (**b**). HCT116 cell line is a chromosomally stable human colorectal cancer cell line and has two alleles of the CAP-H gene (*NCAPH*). The following results indicate that the CAP-H gene was heterozygously tagged in both cell lines.
**a,** Primers located outside of the left (P785) and right (P759) homology arms were used. A 0.72-kb fragment derived from untagged CAP-H was detected for both cell lines #899 and #897 in addition to the fragments from mClover3-CAP-H (4.2 kb) and td5oxStayGold-tagged CAP-H (5.3 kb), respectively. Hyg: hygromycin resistance gene.
**b,** Anti–CAP-H antibody (Proteintech, #11515-1-AP) was used to characterize the size of CAP-H proteins. An 83-kDa band for untagged CAP-H was detected for both cell lines #899 and #897 in addition to those for mClover3-tagged (110 kDa) and td5oxStayGold-tagged (144 kDa) CAP-H proteins, respectively. Anti–β-actin monoclonal antibody (AC-15) was used as a loading control.

# Supplementary Fig. 5

td5StayGold(c4)=GianCreg
td8oxStayGold(c4)=β-tubulin

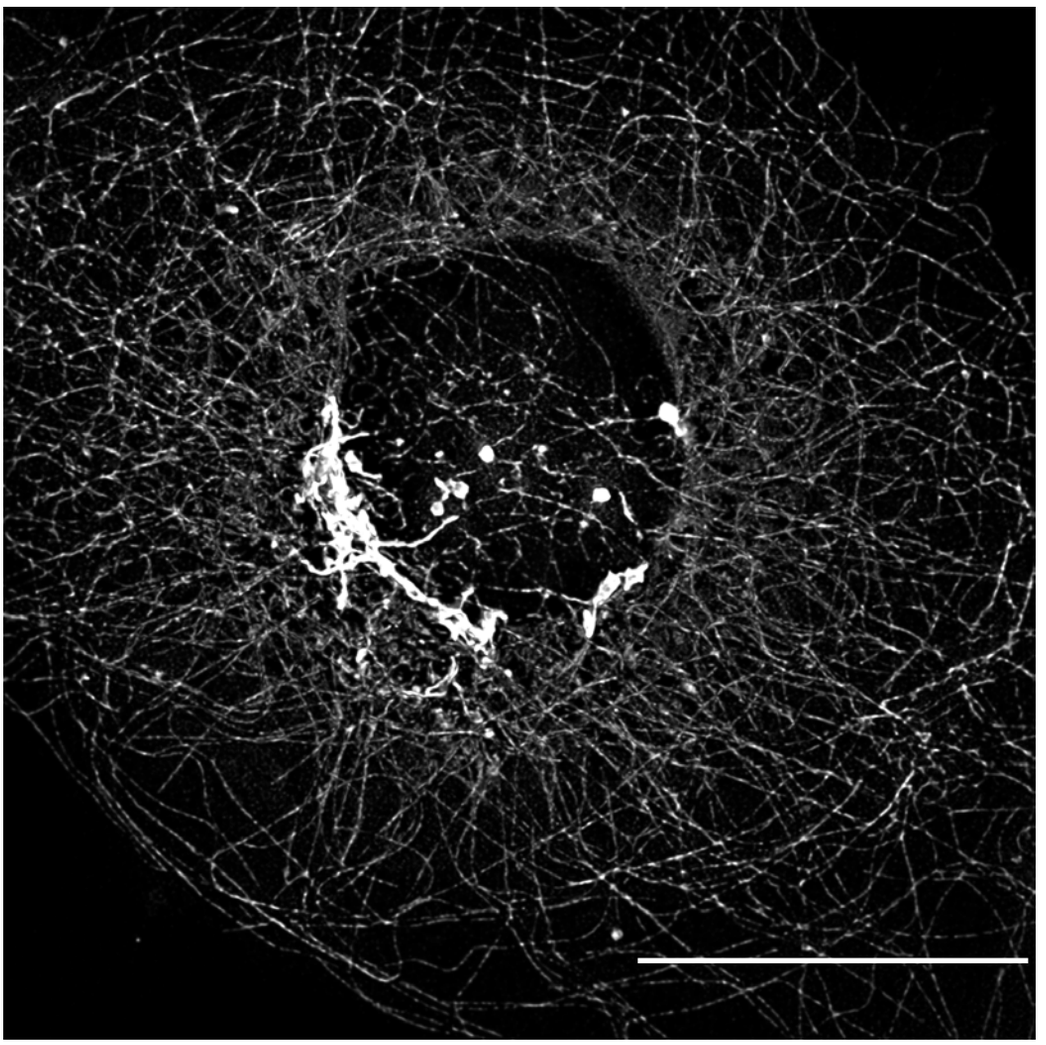

**Supplementary Fig. 5 | Dual-targeting of StayGold variants to the Golgi apparatus and microtubule network.**
COS-7 cells were cotransfected with td5StayGold(c4)=GianCreg and td8ox2StayGold(c4)=β-tubulin. A fine 3D reconstruction of the whole Golgi apparatus with a microtubule network was generated by volumetric imaging (*z*-step, 0.216 μm; *z*-range, 1.94 μm) using the lattice SIM method (Elyra 7). The Leap mode was used. Scale bar, 20 μm. Shown is a representative of $n = 7$ independent experiments (transfections).

# Supplementary Fig. 6

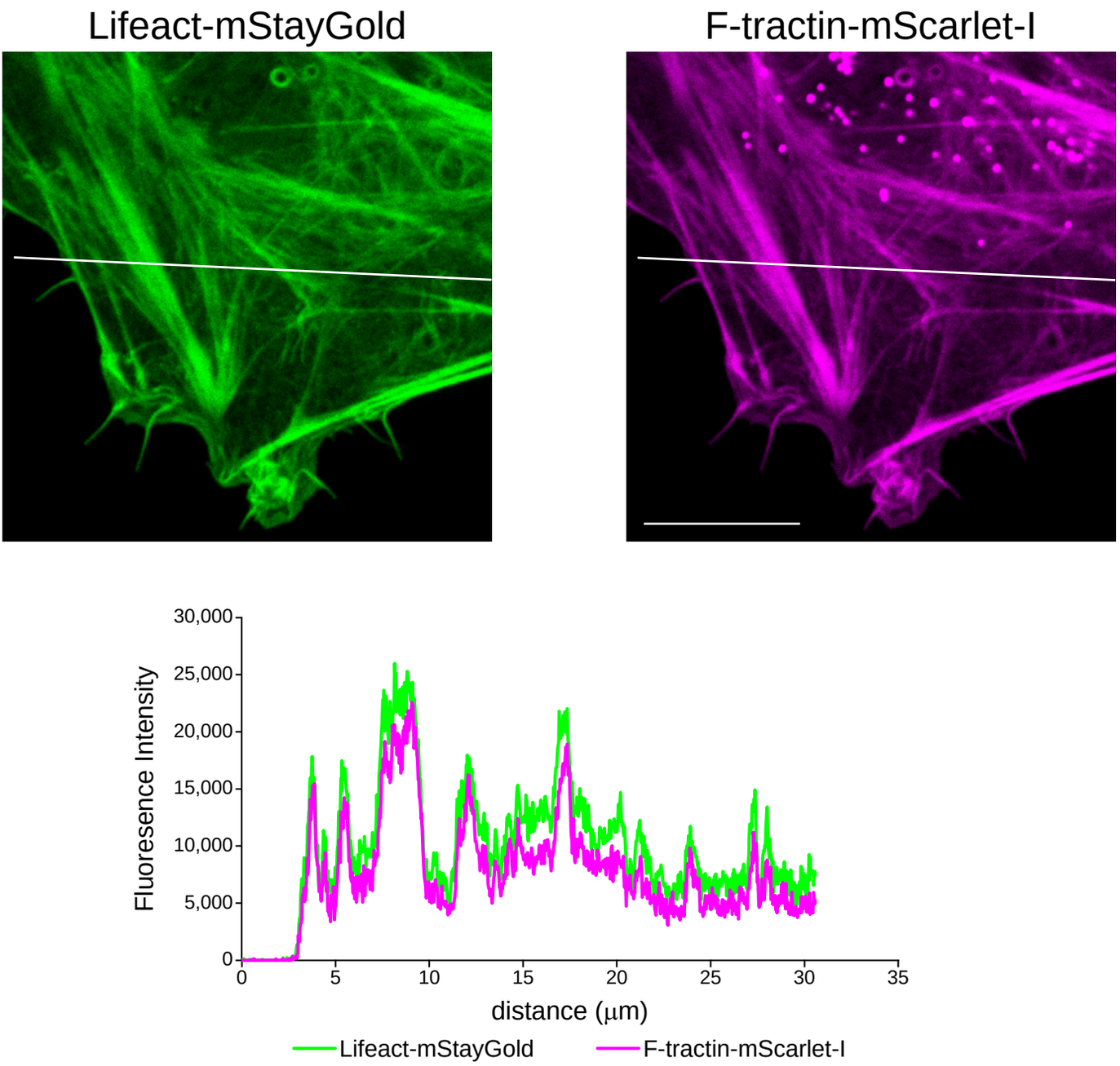


**Supplementary Fig. 6 | Colocalization of Lifeact-mStayGold and F-tractin-mScarlet-I in a Vero cell.**
*top*, CLSM (single-beam) images of Lifeact-mStayGold (left, green channel) and F-tractin-mScarlet-I (right, red channel). Scale bar, 10 μm.
*bottom*, The line profile plots indicate the intensity distribution of green and red channels through the white lines across the cell.

# Supplementary Fig. 7

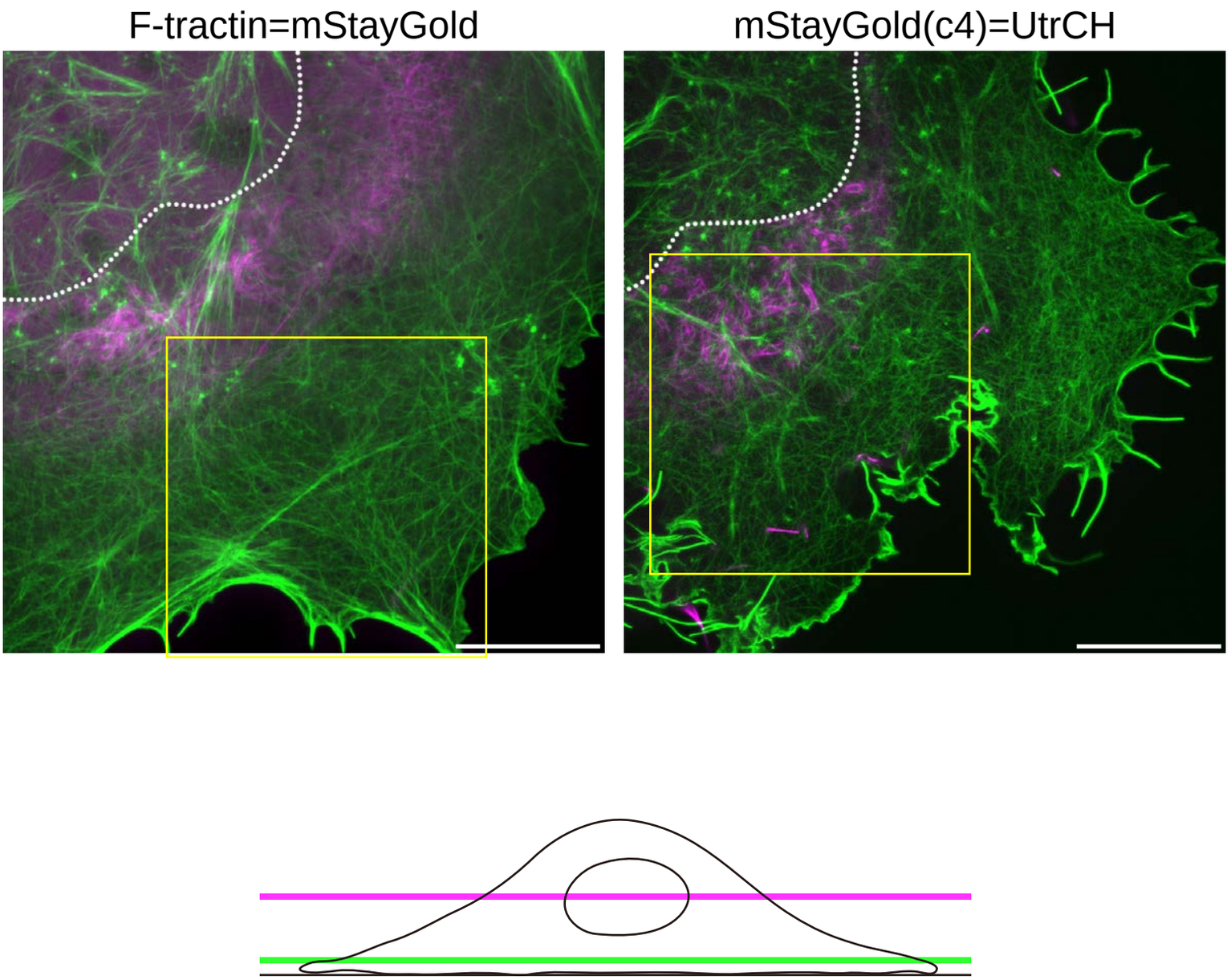


**Supplementary Fig. 7 | F-actin distribution visualized by mStayGold-tagged actin-binding domains.** COS-7 cells expressing F-tractin=mStayGold (left) or mStayGold(c4)=UtrCH (right) were imaged by SDSRM (SpinSR10). UtrCH: utrophin calponin homology domain[28]. For each experiment, a confocal image sectioned nearest the cell bottom is shown in green. Images were acquired continuously at 3.18 frames/s for 5.24 min (boxed regions, Supplementary Video 6). A confocal image sectioned across the center of the nucleus is shown in magenta. The nucleus is delineated by a dotted line. Scale bars, 10 μm. The F-tractin=mSayGold images shown are representative of *n* = 15 independent cell samples. The mStayGold(c4)=UtrCH images shown are representative of *n* = 13 independent cell samples.

# Supplementary Fig. 8

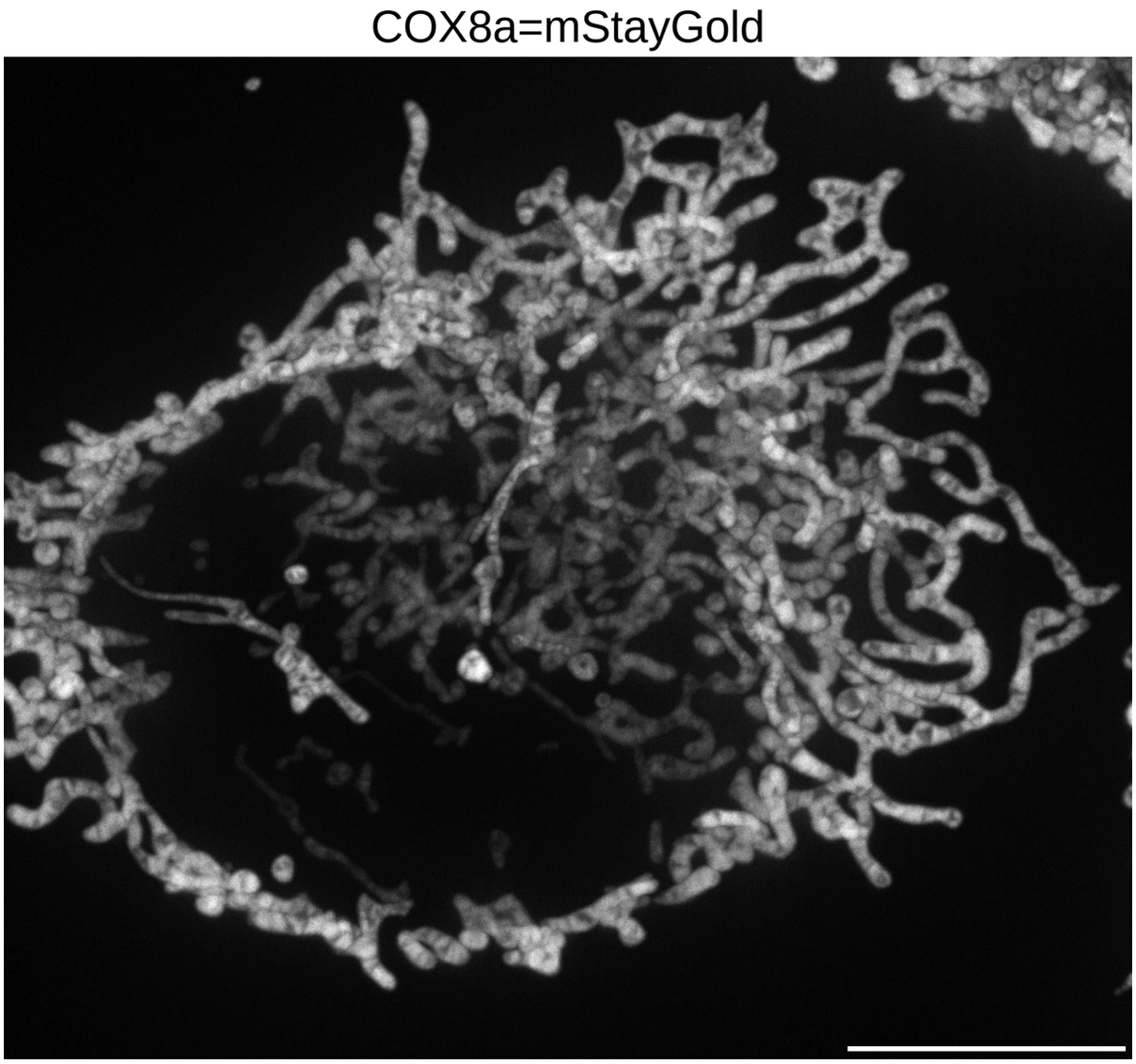


**Supplementary Fig. 8 | A cell-wide 3D reconstruction of the inner mitochondrial membrane.**
HeLa cells constitutively expressing COX8a=mStayGold were volume (*z* step, 0.25 μm; *z* range, 9.0 μm) imaged by SDSRM (SpinSR10) with an exposure time of 200 ms. An MIP image is shown.
Some mitochondria were found along the nuclear tubular invaginations. Scale bar, 10 μm. Shown is a representative of $n = 4$ cell samples.

# Supplementary Table. 1

| | StayGold pH8.5 | StayGold pH5.6 |
|---|---|---|
| **Wavelength (Å)** | 1.0 | 1.0 |
| **Resolution range (Å)** | 91.2 - 1.56 (1.62 - 1.56) | 67.0 - 2.2 (2.28 - 2.2) |
| **Space group** | P $2_1$ | P $6_1$ |
| **Unit cell** | 53.9 Å 44.9 Å 93.8 Å 90° 103.4° 90° | 134.0 Å 134.0 Å 59.0 Å 90° 90° 120° |
| **Total reflections** | 335808 (28363) | 325103 (19041) |
| **Unique reflections** | 61988 (5842) | 30868 (3015) |
| **Multiplicity** | 5.4 (4.9) | 10.5 (6.3) |
| **Completeness (%)** | 99.2 (93.0) | 99.8 (98.1) |
| **Mean I/sigma(I)** | 8.85 (0.46) | 10.97 (2.77) |
| **Wilson B-factor** | 17.48 | 14.25 |
| **R-merge** | 0.06797 (0.4089) | 0.1706 (0.4423) |
| **R-meas** | 0.07498 (0.4577) | 0.1794 (0.4842) |
| **R-pim** | 0.03111 (0.2015) | 0.05485 (0.1913) |
| **CC1/2** | 0.999 (0.91) | 0.994 (0.85) |
| **CC*** | 1.000 (0.976) | 0.998 (0.958) |
| **Reflections used in refinement** | 61893 (5759) | 30858 (3015) |
| **Reflections used for R-free** | 1986 (197) | 1994 (192) |
| **R-work** | 0.1863 (0.3585) | 0.1547 (0.2039) |
| **R-free** | 0.2153 (0.3804) | 0.1897 (0.2869) |
| **CC(work)** | 0.967 (0.869) | 0.968 (0.888) |
| **CC(free)** | 0.956 (0.824) | 0.951 (0.833) |
| **Number of non-hydrogen atoms** | 4160 | 4043 |
| **macromolecules** | 3475 | 3488 |
| **ligands** | 40 | 63 |
| **solvent** | 663 | 492 |
| **Protein residues** | 424 | 425 |
| **RMS(bonds)** | 0.002 | 0.002 |
| **RMS(angles)** | 0.54 | 0.62 |
| **Ramachandran favored (%)** | 98.55 | 97.12 |
| **Ramachandran allowed (%)** | 1.45 | 2.88 |
| **Ramachandran outliers (%)** | 0.00 | 0.00 |
| **Rotamer outliers (%)** | 0.54 | 1.05 |
| **Clashscore** | 2.99 | 2.77 |
| **Average B-factor (Å²)** | 22.63 | 15.56 |
| **macromolecules (Å²)** | 19.57 | 14.09 |
| **ligands (Å²)** | 13.83 | 13.61 |
| **solvent (Å²)** | 32.87 | 26.23 |

**Supplementary Table. 1 | Data collection and refinement statistics.**
Statistics for the highest-resolution shell are shown in parentheses.

**Supplementary Video captions**

**Supplementary Video 1 | Visualization of chromosome-targeting of td5oxStayGold-tagged condensin I at low copy number expressed via a genome-editing technique.** After release from cell cycle arrest, genome-edited HCT116 cells (#897) were imaged for CAP-H-td5oxStayGold (at 488 nm excitation) and SiR-DNA-labeled chromosomes (at 637 nm excitation) using spinning-disk LSCM (SpinSR10) at the indicated times (hour: min). Every 1 min, 3D scanning was executed with a *z*-step size of 1 μm over an axial range of 13 μm, and the green and far-red fluorescence images were merged. Maximum intensity projection (MIP) images are shown. This movie (6.20 MB) has been generated via considerable compression of the original large-volume video data (1.52 GB). Compression was made using TMPGEnc. See Fig. 4. Shown is a representative of $n = 3$ independent experiments.

**Supplementary Video 2 | High-speed visualization of chromosome-targeting of td5oxStayGold-tagged condensin I in genome-edited HCT116 cells.** After release from cell cycle arrest, genome-edited HCT116 cells (#897) were imaged at a single *z* position for observing CAP-H-td5oxStayGold (488 nm excitation) and for SiR-DNA-labeled chromosomes (637 nm excitation) by spinning-disk LSCM (SpinSR10) at 1 frame per second. Merged images at the indicated times (min: s). This movie (9.05 MB) has been generated via considerable compression of the original large-volume video data (7.03 GB). Compression was made using FFmpeg. See Extended Data Fig. 5a.

**Supplementary Video 3 | Photostability comparison between CAP-H-mClover3 and CAP-H-td5oxStayGold under the same optical conditions.** Genome-edited HCT116 cells (#899, left vs. #897, right) during prometaphase were volume (*z* step, 0.25 μm; *z* range, 2.5 μm) imaged by spinning-disk LSCM (SpinSR10) with excitation at 488 nm continuously every 6.9 sec over a total period of 278 sec. MIP images are shown. This movie (1.40 MB) has been generated via considerable compression of the original large-volume video data (12.4 MB). Compression was made using TMPGEnc. Elapsed times (min: s). See Extended Data Fig. 5b.

**Supplementary Video 4 | Visualization of td5StayGold-harboring Golgi membranes.** Volumetric and continuous imaging of HeLa cells expressing td5StayGold(c4)=GianCreg in two independent experiments (top and bottom). Cells were volume (*z* step, 0.5 μm; *z* range, 2.5 μm) imaged by SDSRM (SpinSR10)

continuously with an exposure time of 100 ms without using the *z*-drift compensator (IX3-ZDC2, Evident). MIP images are shown. This movie (9.88 MB) has been generated via considerable compression of the original large-volume video data (122 MB). Compression was made using TMPGEnc. Elapsed times (min: s). See Fig. 5b.

**Supplementary Video 5 | Visualization of the Golgi apparatus and microtubule network.** A COS-7 cell expressing td5StayGold(c4)=GianCreg and td8ox2StayGold(c4)=β-tubulin was volume (*z* step, 0.5 μm; *z* range, 1.5 μm) imaged by SDSRM (SpinSR10) continuously with an exposure time of 200 ms without using the *z*-drift compensator (IX3-ZDC2, Evident). MIP images are shown. This movie (9.43 MB) has been generated via considerable compression of the original large-volume video data (100 MB). Compression was made using TMPGEnc. Elapsed times (min: s).

**Supplementary Video 6 | Visualizing F-actin dynamics by continuous, sustainable, cell-wide imaging.** COS-7 cells expressing F-tractin=mStayGold (left) or mStayGold(c4)=UtrCH by imaged by SDSRM (SpinSR10) at a single *z* position at 3.18 frames/s for 5.24 min. Elapsed times (min: s). This movie (9.05 MB) has been generated via considerable compression of the original large-volume video data (7.03 GB). Compression was made using TMPGEnc. See Supplementary Fig. 7.

**Supplementary Video 7 | Visualizing the effects of drugs on F-actin organization.** COS7 cells expressing F-tractin=mStayGold (top) or mStayGld(c4)=UtrCH (bottom) were imaged by SDSRM (SpinSR10) at a single z position at 2.41 frames/s for 13.82 min. Cells were treated with 1 μM Cytochalasin D (left) or 2 μM Latrunculin A (right). Elapsed times (min: s). This movie (9.38 MB) has been generated via considerable compression of the original large-volume video data (4.29 GB). Compression was made using FFmpeg. See Extended Data Fig. 7.

**Supplementary Video 8 | Visualizing the inner mitochondrial membrane dynamics by sustainable, cell-wide volumetric SIM imaging.** HeLa cells expressing COX8a=mStayGold were 3D scanned continuously with a *z*-step size of 0.11 μm over an axial range of 2.08 μm by lattice SIM (Elyra 7) at 37 °C. The total number of acquired volumes was 47. SIM$^2$ was used for image reconstruction. This movie (6.69 MB) has been generated via considerable compression of the original large-volume video data (47 MB). Compression was made using TMPGEnc. Elapsed times (min: s). See Fig. 5c.

**Supplementary Video 9 | Visualizing the inner mitochondrial membrane dynamics by fast, sustainable imaging.** HeLa cells expressing COX8a=mStayGold were imaged by SDSRM (SpinSR10). Single-plane images were acquired continuously at 8.70 frames/s (exposure time: 100 ms). This movie highlights stable mitochondria. The autofocus function of a *z*-drift compensator (IX3-ZDC2, Evident) was continuously active. The total number of acquired frames was 1,000. This movie (6.71 MB) has been generated via considerable compression of the original large-volume video data (70.7 MB). Compression was made using TMPGEnc. Elapsed times (min: s). The stable IMM dynamics shown is a representative of $n = 17$ cells over $n = 10$ independent transfections.

**Supplementary Video 10 | Visualizing the inner mitochondrial membrane dynamics by fast, sustainable imaging.** HeLa cells expressing COX8a=mStayGold were imaged by SDSRM (SpinSR10). Single-plane images were acquired continuously at 2.41 frames/s (exposure time: 400 ms). This movie highlights a mobile mitochondrium. The autofocus function of a *z*-drift compensator (IX3-ZDC2, Evident) was continuously active. The total number of acquired frames was 500. This movie (3.19 MB) has been generated via considerable compression of the original large-volume video data (31.4 MB). Compression was made using TMPGEnc. Elapsed times (min: s). The mobile IMM dynamics shown is a representative of $n = 14$ cells over $n = 9$ independent transfections.

**Supplementary Video 11 | Agonist-, antagonist-, and $Ca^{2+}$ ionophore-induced longitudinal changes in IMM structures revealed by fast, sustained, wide imaging.** HeLa cells expressing COX8a=mStayGold were imaged by SDSRM (SpinSR10) continuously at a temporal resolution of 2.5 frames per second. Two representative experimental data are shown. Histamine, cyproheptadine, and ionomycin were applied at 1 minute, 2.5 minutes, and 4 minutes, respectively. The autofocus function of a *z*-drift compensator (IX3-ZDC2, Evident) was continuously active. This movie (8.9 MB) has been generated via considerable compression of the original large-volume video data (412 MB). Compression was made using TMPGEnc. Elapsed times (min: s). See Extended Data Fig. 8. Representatives of $n = 12$ independent experiments (transfections).